Molecular Cancer Therapeutics

^{177}Lu-EC0800 Combined with the Antifolate Pemetrexed: Preclinical Pilot Study of Folate Receptor Targeted Radionuclide Tumor Therapy

Josefine Reber[1], Stephanie Haller[1], Christopher P. Leamon[2], and Cristina Müller[1]

Abstract

Targeted radionuclide therapy has shown impressive results for the palliative treatment of several types of cancer diseases. The folate receptor has been identified as specifically associated with a variety of frequent tumor types. Therefore, it is an attractive target for the development of new radionuclide therapies using folate-based radioconjugates. Previously, we found that pemetrexed (PMX) has a favorable effect in reducing undesired renal uptake of radiofolates. Moreover, PMX also acts as a chemotherapeutic and radiosensitizing agent on tumors. Thus, the aim of our study was to investigate the combined application of PMX and the therapeutic radiofolate ^{177}Lu-EC0800. Determination of the combination index (CI) revealed a synergistic inhibitory effect of ^{177}Lu-EC0800 and PMX on the viability of folate receptor–positive cervical (KB) and ovarian (IGROV-1) cancer cells *in vitro* (CI < 0.8). In an *in vivo* study, tumor-bearing mice were treated with ^{177}Lu-EC0800 (20 MBq) and a subtherapeutic (0.4 mg) or therapeutic amount (1.6 mg) of PMX. Application of ^{177}Lu-EC0800 with PMX_{ther} resulted in a two- to four-fold enhanced tumor growth delay and a prolonged survival of KB and IGROV-1 tumor-bearing mice, as compared to the combination with $PMX_{subther}$ or untreated control mice. $PMX_{subther}$ protected the kidneys from undesired side effects of ^{177}Lu-EC0800 (20 MBq) by reducing the absorbed radiation dose. Intact kidney function was shown by determination of plasma parameters and quantitative single-photon emission computed tomography using ^{99m}Tc-DMSA. Our results confirmed the anticipated dual role of PMX. Its unique features resulted in an improved antitumor effect of folate-based radionuclide therapy and prevented undesired radio-nephrotoxicity. *Mol Cancer Ther; 12(11); 2436–45. ©2013 AACR.*

Introduction

Targeted radionuclide therapy has shown impressive results for the palliative treatment of several cancer diseases. It is based on the use of particle-emitting radioisotopes (e.g., ^{177}Lu, ^{90}Y, ^{131}I) in conjunction with tumor-targeted biomolecules (e.g., peptides, antibodies; ref. 1). A prominent example of a successfully used radiopharmaceutical in clinical routine are somatostatin-based radiopeptides (e.g., ^{177}Lu-DOTATATE, ^{90}Y-DOTATOC) for the treatment of neuroendocrine tumors (2). Moreover, radiolabeled antibodies such as ^{90}Y-Ibritumomab (Zevalin) and ^{131}I-tositumomab (Bexxar) are approved for the treatment of non-Hodgkins lymphoma (3).

The development of new targeting strategies for the treatment of further tumor types is of high interest and would have a critical impact on the future management of these cancer diseases. In this respect, the folate receptor is an attractive target as it has been identified as specifically associated with a variety of cancer types, such as ovarian, endometrial, lung, brain, breast, and colorectal cancer (4, 5). The vitamin folic acid has been used as a targeting ligand because it binds to the folate receptor with high affinity followed by endocytotic internalization of the therapeutic payload into cancer cells (6). While folic acid conjugates of highly toxic chemotherapeutics have been successfully used in clinical trials (7, 8), application of therapeutic folic acid radioconjugates is currently being developed in preclinical studies.

Substantial expression of the folate receptor in the proximal tubule cells of the kidneys results in commonly high and specific renal uptake of folate-based radioconjugates (9, 10). As a consequence there is an inherent risk of damage to the kidneys by particle radiation. However, we have shown in several preclinical studies that administration of the antifolate pemetrexed (PMX) resulted in a tremendous reduction of the radiofolate's retention in the kidneys whereas accumulation in tumor xenografts remained unaffected (11–13). The exact mechanism of this interaction is still not completely clear.

Authors' Affiliations: [1]Center for Radiopharmaceutical Sciences ETH-PSI-USZ, Paul Scherrer Institute, Villigen-PSI, Switzerland; [2]Endocyte Inc., West Lafayette, Indiana

Note: Supplementary data for this article are available at Molecular Cancer Therapeutics Online (http://mct.aacrjournals.org/).

Corresponding Author: Cristina Müller, Center for Radiopharmaceutical Sciences ETH-PSI-USZ, Paul Scherrer Institute, 5232 Villigen-PSI, Switzerland. Phone: 41-56-310-44-54; Fax: 41-56-310-28-49; E-mail: cristina.mueller@psi.ch

doi: 10.1158/1535-7163.MCT-13-0422-T

However, in numerous preclinical studies, we observed an interrelation between the kidney reducing effect and the time point of preinjected PMX (14) as well as the molar amount of PMX and the folate radioconjugate, respectively (15). However, the reduced kidney uptake of radiofolates was not a result of PMX's antifolate activity as the effect was maintained even if PMX was applied in combination with the antidote thymidine (16). These facts suggest that PMX's kidney reducing effect is based on a competition among PMX and the folate radioconjugate for folate receptor binding sites in the kidneys.

PMX is a multitargeted antifolate, which is clinically approved for the treatment of pleural mesothelioma and non–small cell lung cancer in combination with cisplatin (17–19). Moreover, PMX is currently being tested in a number of clinical trials for the treatment of several other cancer types (reviewed in ref. 20), among those is also ovarian cancer (21). PMX has been used in combinations with gemcitabine, tyrosine kinase inhibitors, antibodies, or even external radiation (22–24). A combination of PMX with external radiotherapy was based on the observation that PMX acts as a radiosensitizing agent in variable types of cancer cells *in vitro* and *in vivo* (25–28).

We hypothesized that PMX would have a dual role if it was combined with therapeutic folate radioconjugates. First, it was expected to prevent radionephropathy by reducing the absorbed radiation dose of folate radioconjugates in the kidneys. Second, PMX was believed to enhance the therapeutic efficacy of folate-based radionuclide tumor therapy by its action as a chemotherapeutic and radiosensitizing agent.

The goal of this study was to show the anticipated dual role of PMX. For this purpose, we used an established DOTA-folate conjugate (EC0800; ref. 29), which was radiolabeled with ^{177}Lu ($T_{1/2} = 6.7$ days, $E_{av(\beta^-)}$: 134 keV, $E_{(\gamma)}$: 113 keV, 208 keV). ^{177}Lu-EC0800 was applied in combination with PMX using 2 folate receptor positive human cancer cells (KB and IGROV-1) *in vitro* and as human tumor xenografts in athymic nude mice. Moreover, the protective effect of PMX on the kidneys to reduce the absorbed radiation dose was investigated in non–tumor-bearing mice.

Materials and Methods

Preparation of ^{177}Lu-EC0800

The DOTA-folate conjugate (EC0800; ref. 29) was kindly provided by Endocyte Inc. (Supplementary Fig. S1). The radiosynthesis of ^{177}Lu-EC0800 and the evaluation of its stability were carried out as previously reported (Supplementary Methods; ref. 30). It was shown that ^{177}Lu-EC0800 was stable (>95%) over at least 24 hours in PBS and human blood plasma.

Cell culture

KB cells (human cervical carcinoma cells, ACC-136), and PC-3 (human prostate carcinoma cells, ACC-465) were purchased from the German Collection of Microorganisms and Cell Cultures (DSMZ). IGROV-1 cells (human ovarian carcinoma cells) were a kind gift from Dr. Gerrit Jansen (Department of Rheumatology, VU University Medical Center, Amsterdam, the Netherlands). All 3 cell lines were authenticated by DMSZ based on DNA profiling. KB and IGROV-1 cells are known to express the folate receptor (31, 32), whereas folate receptor negative PC-3 cells (33) were used as a negative control. PC-3 cells were cultured in RPMI 1640 medium (Amimed) whereas KB and IGROV-1 cells were cultured in folate-free RPMI medium referred to as FFRPMI (without folic acid, vitamin B_{12}, and phenol red; Cell Culture Technologies GmbH). Cell culture media were supplemented with 10% fetal calf serum, L-glutamine, and antibiotics (penicillin/streptomycin/fungizone). Routine culture treatment was conducted twice a week. Uptake and internalization studies of ^{177}Lu-EC0800 as well as clonogenic and MTT assays were conducted as previously reported in the literature in detail in the Supplementary Methods (29, 34).

MTT assay

Cell viability was assessed using an MTT assay (35). In brief, KB, IGROV-1, and PC-3 cells were treated with 200 μL FFRPMI medium (without supplements) containing ^{177}Lu-EC0800 (0.001–5.0 MBq/mL) and/or PMX (0.01–100 μmol/L; pemetrexed, Alimta, LY231514; Eli Lilly, Supplementary Fig. S1). The control cells were incubated with FFRPMI medium only. After 4 hours incubation at 37°C, the cells were washed once with 200 μL PBS followed by addition of FFRPMI or RPMI medium (with supplements). Cells were then allowed to grow for 4 days at 37°C without changing medium. Analysis of the viability was conducted as previously reported using an MTT reagent and a microplate reader (Victor X3; Perkin Elmer; ref. 36). To quantify cell viability, the absorbance of the test samples was expressed as percentage of the absorbance of the control cell samples (=100%). Dose–response curves were analyzed using the software *GraphPad Prism* (version 4.0). Inhibition of cell viability was expressed as the half-maximal inhibitory concentration of PMX (IC_{50} in μmol/L) and as the half-maximal inhibitory activity concentration of ^{177}Lu-EC0800 (IAC_{50} in MBq/mL) by measuring dose–response curves of PMX and ^{177}Lu-EC0800. The dose–response curves were used to determine the combination index (CI) according to Chou and colleagues (Supplementary Methods; ref. 37).

Animal studies

The *in vivo* experiments were approved by the local veterinarian department and conducted in accordance with the Swiss law of animal protection. Female athymic nude mice (4–5 week-old CD-1 Foxn-1/nu; Charles River Laboratories) were fed with a folate-deficient rodent diet (Harlan Laboratories) starting 5 days before tumor cell inoculation (38). For therapy experiments, endpoint criteria were defined as (i) a tumor volume >1000 mm^3, (ii)

body weight loss of >15%, (iii) active ulceration of the tumor xenograft, or (iv) abnormal behavior of the mice and signs of unease.

Biodistribution study and dosimetric calculations

Biodistribution studies over 72 hours were conducted as previously reported (Supplementary Methods and Table S1; ref. 29). These datasets were used to estimate the equivalent absorbed radiation dose to the tumor xenografts and kidneys upon injection of ^{177}Lu-EC0800 (Supplementary Methods). Based on the biodistribution results the accumulation of radioactivity in KB and IGROV-1 tumors was taken as equal. For estimation of the kidney dose, it was assumed that in the case of preinjected PMX kidney uptake was reduced to 25% of control values.

Biodistribution studies conducted with ^{3}H-PMX are reported in the Supplementary Methods.

Investigation of potential radiotoxicity

Groups of 6 mice were injected with only PBS (group A), with ^{177}Lu-EC0800 (20 MBq, 1 nmol; group B) or with ^{177}Lu-EC0800 (20 MBq, 1 nmol) and $PMX_{subther}$ (0.4 mg; group C). From day 21 after start of the therapy, the animals were fed with a standard rodent diet. For studying plasma parameters, blood was taken from the sublingual vein collected in heparinized vials at day 50, 130, and 180 or before euthanasia. Blood plasma parameters such as creatinine, blood urea nitrogen, alkaline phosphatase, and total bilirubin were determined using a Fuji Dri-Chem 40000i analyzer (Polymed Medical Center AG). Quantitative single-photon emission computed tomography (SPECT) to determine renal uptake of ^{99m}Tc-DMSA in mice was conducted in week 3, 15, and 23 of the experiment.

SPECT experiments were conducted with a 4-head multiplexing multi-pinhole camera (NanoSPECT/CT; Bioscan Inc.) using collimators of 4 × 9 holes of a diameter of 1.4 mm. Dimercaptosuccinic acid (DMSA)-kits (TechneScan) were purchased from Mallinckrodt Inc. The ^{99m}Tc-radiolabeling was conducted according to the instructions of the manufacturer using ^{99m}Tc-pertechnetate, which was freshly eluted from a ^{99m}Tc-generator (Mallinckrodt Inc.). SPECT images of the kidneys (30-mm scan length) were acquired 2 hours after injection of ^{99m}Tc-DMSA (~30 MBq/mouse). After acquisition, SPECT data were reconstructed iteratively with HiSPECT software (version 1.4.3049; Scivis GmbH) using a γ-energy of 140 keV for ^{99m}Tc. Quantification of renal uptake of ^{99m}Tc-DMSA was carried out as previously reported using InVivoScope postprocessing software (version 2.0; Bioscan Inc.; ref. 39).

Therapy studies in tumor-bearing mice

Twenty mice were inoculated with KB tumor cells (4.5×10^6 in 100 μL PBS, model I) and another 20 mice were inoculated with IGROV-1 tumor cells (6.0×10^6 in 100 μL PBS, model II). At the start of the therapy 4 days later, the average tumor size reached a volume of ~65 mm^3 (KB xenografts) and ~40 mm^3 (IGROV-1 xenografts). For each study, 4 groups of 5 mice were injected with only PBS (group A), with 2 × 0.8 mg PMX (i.e., PMX_{ther}, group B), with 1 × 20 MBq ^{177}Lu-EC0800 combined with 1 × 0.4 mg PMX (i.e., $PMX_{subther}$, group C), and with 1 × 20 MBq ^{177}Lu-EC0800 combined with 2 × 0.8 mg PMX (i.e., PMX_{ther}, group D).

Body weights and tumor volumes were measured 3 times a week. The tumor volume (V) was determined by measuring 2 perpendicular diameters with a digital caliper and calculated by using the formula $V = [0.5 \times (L \times W^2)]$, where L is the length of the tumor (large diameter) and W is the width (small diameter; ref. 40). The values were indicated as the average of the individual relative tumor volumes ($RTV = V_x/V_0$; V_x = volume at day x, V_0 = volume at day 0) and of individual relative body weight ($RBW = W_x/W_0$; W_x = weight at day x; W_0 = weight at day 0). The therapeutic efficacy was expressed as the percentage of tumor growth inhibition ($\%TGI = 100 - (T/C \times 100)$, where T is the mean RTV of the treated mice and C is the mean RTV of untreated control mice at day 17 when the first mouse in the control group was euthanized. Tumor growth delay (TGD) was calculated for the time that passed until the RTVs reached 4-fold the value of day 0. The tumor growth delay index (TGDI) was calculated as the ratio of TGDs among treated animals and control animals (41).

Statistical analysis

Statistics was conducted by using a t-test (Microsoft Excel software). All analyses were 2-tailed and considered as type 3 (2 sample unequal variance). A P-value of <0.05 was considered as statistically significant.

Results

Cancer cell lines

The human cervical KB cancer cell line is a subclone of HeLa cells (42), known to express the folate receptor at very high levels. IGROV-1 cells are human ovarian cancer cells that express the folate receptor at a somewhat lower level than KB cells (12, 31, 36). The human prostate cancer cell line PC-3 does not express the folate receptor and was used as a negative control. These facts were confirmed in uptake/internalization studies of ^{177}Lu-EC0800 (Supplementary Fig. S2).

Cell survival upon exposure to ^{177}Lu-EC0800

Clonogenic assays revealed plating efficiencies of 11%, 14%, 18% and 16%, for KB, IGROV-1, and PC-3 cells. At a radioactivity concentration of 1.0 MBq/mL ^{177}Lu-EC0800 (16 nmol/L) with a 4 hours exposure, the survival fraction of KB and IGROV-1 cells was 0.12 and 0.43, respectively. The survival fraction of folate receptor negative PC-3 cells was still 0.98, even after the treatment with a 5-fold higher radioactivity concentration. Reduction of cell survival was completely suppressed by preincubating folate

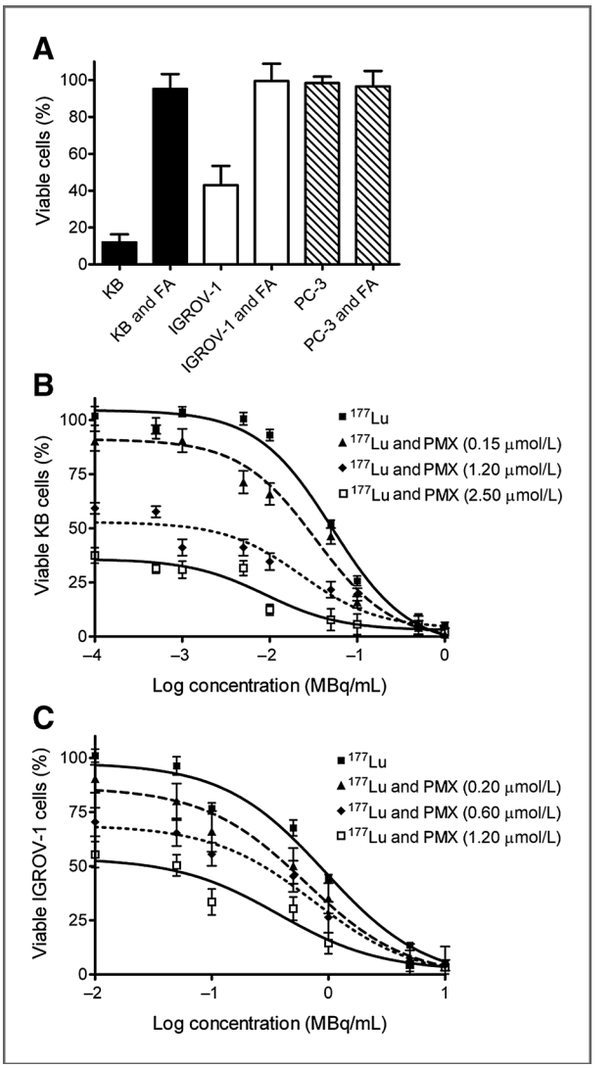

Figure 1. A, survival of folate receptor–positive KB and IGROV-1 cells and folate receptor–negative PC-3 cells upon exposure to ^{177}Lu-EC0800 (1 MBq/mL; 16 nmol/L) in the presence and absence of excess folic acid (FA). B and C, dose–response curves of KB and IGROV-1 tumor cells incubated with variable activity concentrations of ^{177}Lu-EC0800 (indicated as ^{177}Lu) and PMX.

receptor positive tumor cells with excess folic acid to block folate receptors (Fig. 1A; Supplementary Fig. S3).

Cell viability upon exposure of ^{177}Lu-EC0800 combined with PMX

MTT assays were conducted to determine IAC_{50} and IC_{50} values of ^{177}Lu-EC0800 and PMX. The inhibition of cell viability was found to be dependent on the concentration of PMX in all cell lines. The IC_{50} value of PMX amounted to 1.22 ± 0.13 μmol/L and 0.93 ± 0.17 μmol/L for KB and IGROV-1 cells, respectively. The IAC_{50}-values of ^{177}Lu-EC0800 revealed activity concentrations of 0.054 ± 0.004 MBq/mL for KB and 0.83 ± 0.08 MBq/mL for IGROV-1 tumor cells (Fig. 1B and C).

Combination index

The interactions between ^{177}Lu-EC0800 and PMX were calculated according to the results obtained with KB and IGROV-1 cells, which were exposed to ^{177}Lu-EC0800 and PMX as single agents or simultaneously. The concentrations of the test agents, alone and in combination, required to reduce cell viability to 55% and 70% of controls were determined. All calculations revealed values of the CI below 0.8, indicating a synergistic effect between ^{177}Lu-EC0800 and PMX (Supplementary Table S2).

Biodistribution studies

Biodistribution studies in KB and IGROV-1 tumor-bearing mice showed a relatively high uptake of ^{177}Lu-EC0800 in tumor xenografts [KB: 5.94 ± 1.20% ID/g and IGROV-1: 6.58 ± 1.50% ID/g; 4 hours past injection (p.i)], and a ∼10-fold higher accumulation in the folate receptor positive kidneys. PMX treatment reduced renal uptake of ^{177}Lu-EC0800 up to 7-fold, while simultaneously allowing for greater tumor uptake (Table 1). Dosimetric estimation revealed a dose of 0.38 Gy/MBq to the tumor xenografts and 4.84 Gy/MBq to the kidneys if ^{177}Lu-EC0800 was applied as a single agent. Under the assumption of a 4-fold reduced renal uptake of ^{177}Lu-EC0800 in combination with PMX, the kidney dose was reduced to 1.21 Gy/MBq whereas the tumor dose remained unaffected (Supplementary Methods and Fig. S4).

Short after injection of ^{3}H-PMX, the uptake in the kidneys was relatively high (∼2.7% ID/g, 1 hour p.i.) but a significant washout was observed within the following hour (∼0.8% ID/g, 2 hours p.i.). In the tumor tissue accumulation of ^{3}H-PMX was low (∼1.1% ID/g, 1 hour p.i.) but more constant (0.6% ID/g, 2 hours p.i.) over time (Supplementary Methods and Fig. S5).

Investigation of potential radiotoxicity

In a separate study, radiotoxicity of ^{177}Lu-EC0800 and the kidney protective effect of a subtherapeutic amount of PMX (0.4 mg) were investigated. Nontumor-bearing nude mice were monitored over 6 months. The kidney dose of ^{177}Lu-EC0800 (20 MBq/mouse) was ∼97 Gy (group B). If $PMX_{subther}$ was preinjected, the kidney dose was significantly reduced to ∼24 Gy (group C). At day 50 of the study, plasma parameters of treated mice (groups B/C) were in the same range as those of control mice (group A). However, at day 130, levels of blood urea nitrogen, alkaline phosphatase, and total bilirubin from mice treated with ^{177}Lu-EC0800 (group B) differed significantly from those of control mice (group A). The values obtained from mice of group C were in the same range as the values from mice of group A. Determination of blood plasma parameters at day 180 showed the same result as found at day 130 (Table 2).

The extent of accumulated ^{99m}Tc-DMSA in the kidneys is a measure for tubular function (43). It has previously been used as a valuable *in vivo* tool for monitoring kidney function during radionuclide therapy (39). In week 3, baseline measurements of ^{99m}Tc-DMSA uptake in the

Table 1. Biodistribution data 4 hours after injection of ^{177}Lu-EC0800 (3 MBq, 1 nmol) in KB (model I) and IGROV-1 tumor-bearing nude mice (model II)

	^{177}Lu-EC0800 (model I)		
	Control	**PMX$_{subther}$[a]**	**PMX$_{ther}$[b]**
Blood	0.08 ± 0.01	0.06 ± 0.01	0.06 ± 0.01
Liver	6.61 ± 1.04	4.28 ± 0.69	3.46 ± 0.38
Kidneys	51.0 ± 6.6	9.66 ± 1.14	8.12 ± 0.88
Tumor	5.94 ± 1.20	7.83 ± 0.98	9.01 ± 1.60
Tumor-to-blood	71.6 ± 19.2	131.1 ± 24.6	161.7 ± 17.3
Tumor-to-liver	0.91 ± 0.22	1.88 ± 0.41	2.64 ± 0.65
Tumor-to-kidney	0.12 ± 0.02	0.86 ± 0.14	1.11 ± 0.16
	^{177}Lu-EC0800 (model II)		
	Control	**PMX$_{subther}$[a]**	**PMX$_{ther}$[b]**
Blood	0.16 ± 0.04	0.08 ± 0.00	0.08 ± 0.02
Liver	7.60 ± 2.04	2.75 ± 0.19	2.37 ± 0.68
Kidneys	67.0 ± 13.4	11.4 ± 1.2	9.30 ± 1.96
Tumor	6.58 ± 1.50	9.30 ± 1.96	9.55 ± 0.88
Tumor-to-blood	42.7 ± 7.8	122.7 ± 28.0	127.9 ± 40.6
Tumor-to-liver	0.88 ± 0.16	3.40 ± 0.78	4.32 ± 1.48
Tumor-to-kidney	0.10 ± 0.02	0.81 ± 0.13	1.04 ± 0.54

NOTE: Data are presented as average ± SD ($n = 3$).
[a]PMX$_{subther}$: 0.4 mg per mouse, injected 1 hour before ^{177}Lu-EC0800.
[b]PMX$_{ther}$: 0.8 mg per mouse, injected 1 hour before ^{177}Lu-EC0800.

kidneys showed no significant difference among groups B and C from control mice of group A (Fig. 2A). However, in week 15 the average % ID per kidney of mice treated with ^{177}Lu-EC0800 only (group B: 4.37 ± 2.6% ID/kidney, 2 hours p.i., $P < 0.005$) was significantly lower than in control mice (group A: 11.74 ± 0.7% ID/kidney, 2 hours

Table 2. Plasma parameters of group A (PBS), group B (20 MBq of ^{177}Lu-EC0800), and group C (20 MBq of ^{177}Lu-EC0800 and 0.4 mg of PMX)

	Day	**Group A PBS**	**Group B ^{177}Lu-EC0800**	**Group C ^{177}Lu-EC0800 and PMX$_{subther}$**
CRE (μmol/L)	50	21 ± 3.4	19 ± 2.1	<18
	130	28 ± 12	58 ± 43	<18
	180[a]	19 ± 0.7	114 ± 62[b]	21 ± 0.7
BUN (mmol/L)	50	8.5 ± 0.9	11.8 ± 2.2[b]	10.0 ± 1.1
	130	9.7 ± 0.6	35.0 ± 9.4[c]	8.61 ± 1.1
	180[a]	8.8 ± 0.6	>49.98[c]	9.09 ± 1.4
ALP (U/L)	50	78 ± 10	83 ± 20	70 ± 8
	130	54 ± 16	132 ± 42[c]	71 ± 18
	180[a]	58 ± 14	123 ± 55[b]	67 ± 23
TBIL (μmol/L)	50	10 ± 1.3	8 ± 1.0	11 ± 1.7
	130	12 ± 1.9	24 ± 11[b]	12 ± 4.5
	180[a]	12 ± 3.2	36 ± 1.9[c]	12 ± 5.0

Abbreviations: CRE, creatinine; BUN, blood urea nitrogen; ALP, alkaline phosphatase; TBIL, total bilirubin.
[a]Group B terminal blood sampling.
[b]$P < 0.05$.
[c]$P < 0.005$.

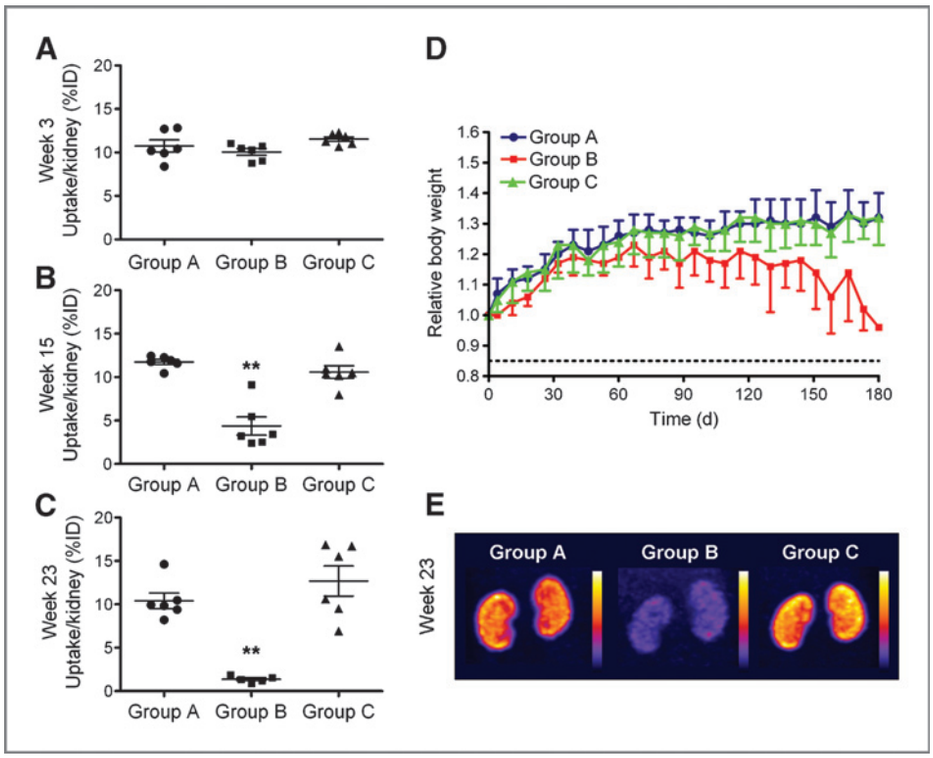

Figure 2. A–C, the average %ID per kidney in week 3, 15, and 23 after injection of ^{99m}Tc-DMSA in untreated control mice (group A), mice treated with ^{177}Lu-EC0800 (group B), and mice treated with ^{177}Lu-EC0800 and PMX$_{subther}$ (group C; **, $P < 0.005$). D, graphs of the relative body weights of mice from each group over the whole time of 6 months. The lowest tolerable body weight is indicated at a relative value of 0.85. E, SPECT images of kidneys after injection of ^{99m}Tc-DMSA of one representative mouse of each group in week 23.

p.i.). Renal uptake of ^{99m}Tc-DMSA in mice that received PMX$_{subther}$ in addition to ^{177}Lu-EC0800 was comparable (group C: 10.58 ± 1.8% ID/kidney, 2 hours p.i., $P = 0.2$) with the value obtained from control animals (Fig. 2B). In week 23 of follow-up, renal accumulation of ^{99m}Tc-DMSA in mice of group B had dropped to 1.38 ± 0.16% ID/kidney 2 hours p.i. ($P < 0.005$), whereas in group C the uptake was still in same range as found for control animals of group A ($P = 0.6$; Fig. 2C).

Constant body weight loss was observed in mice treated with ^{177}Lu-EC0800 (group B) from about day 70 and thereafter. In all cases of group B, the endpoint criterion that required euthanasia was reached before day 180. However, mice that had received PMX$_{subther}$ before the injection of ^{177}Lu-EC0800 (group C) showed body weight gain similar to the untreated controls (group A).

In vivo tumor therapy studies

The injection protocol of the therapy study with KB and IGROV-1 tumor-bearing mice is shown in Fig. 3A. PMX was applied either in a subtherapeutic dose of 0.4 mg (PMX$_{subther}$) or at a therapeutic dose of 2 × 0.8 mg (PMX$_{ther}$) corresponding to 80% of the maximal tolerated dose (MTD). The MTD of PMX was previously determined in mice under the experimental conditions of a folate-free diet and revealed a dose of 2 × 1 mg per mouse (body weight ~ 25 g) with a time lag of 1 week (Supplementary Methods and Fig. S6; ref. 16).

In both tumor models (I and II), constant tumor growth was observed in control mice (group A) where the first mouse reached the endpoint criterion at day 17. For model I, the average RTV in mice treated with PMX$_{ther}$ (group B: 9.8 ± 4.1; $P = 0.90$) and in mice treated with ^{177}Lu-EC0800 and PMX$_{subther}$ (group C: 8.3 ± 3.5, $P = 0.21$) were not significantly different from the average RTV of control mice (group A: 10.0 ± 2.7) at day 17 (Table 3). However, the combined application of ^{177}Lu-EC0800 with PMX$_{ther}$ resulted in a significant decrease of the average RTV (group D: 5.0 ± 2.2; $P < 0.0001$; Fig. 3B). For tumor model II, the average RTV of PMX-treated mice (group B: 27.9 ± 11.8; $P = 0.73$) was not significantly reduced compared to control mice (group A: 30.0 ± 14.9) at the same time point (Table 3). However, a significant reduction of the average RTV was observed in both groups of mice treated with ^{177}Lu-EC0800 (group C: 7.3 ± 3.9, $P = 0.0006$; group D: 2.0 ± 1.7, $P = 0.0002$; Fig. 3C). Monitoring of the body weight revealed slight weight gain over time in model I and a largely constant body weight in model II (Fig. 3D and E). In contrast, pronounced loss of body weight was observed in group B mice of both tumor models (which received PMX$_{ther}$ only). Importantly, the average survival time was increased 75–100% in group D mice from both tumor models compared to group A mice (Table 3).

Discussion

Combining anticancer therapies is a strategy to broaden the therapeutic index by taking an advantage of additive or synergistic antitumor effects and by reducing undesired side effects. This study addressed the question of whether

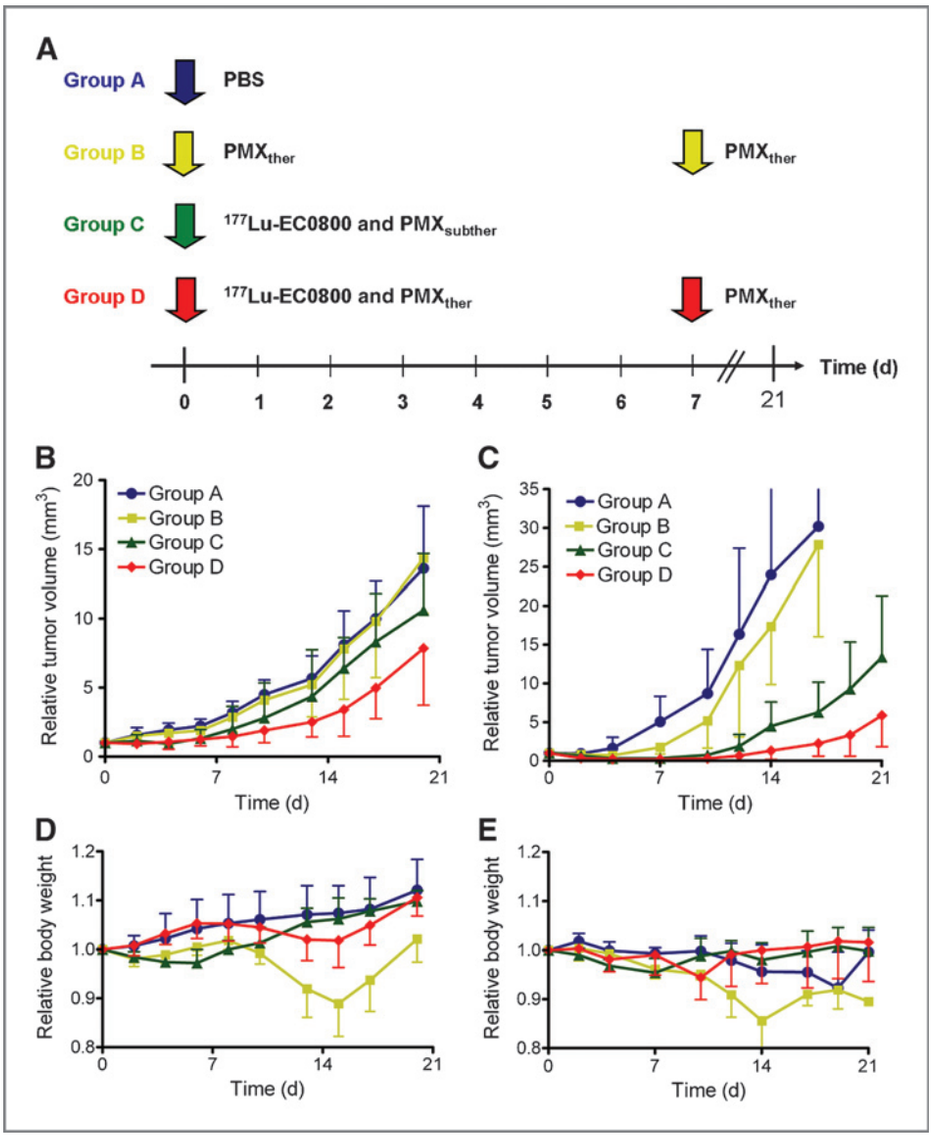

Figure 3. A, injection scheme of the *in vivo* therapy studies conducted in KB (model I) and IGROV-1 tumor-bearing mice (model II). B, graphs of the mean relative tumor volumes of KB tumor xenografts (model I). C, graphs of mean relative tumor volumes of IGROV-1 xenografts (model II). D, graphs of the mean relative body weights of KB tumor-bearing mice (model I). E, graphs of the mean relative body weight of IGROV-1 tumor-bearing mice (model II).

PMX contributes to the antitumor effect of radiofolates and prevents the risk of radionephropathy. *In vitro* the clonogenic potential of KB and IGROV-1 tumor cells was reduced upon exposure to ^{177}Lu-EC0800 in a concentration-dependent manner (Fig. 1). Moreover it was proven that this effect was specifically folate receptor mediated. It was more pronounced in KB cells, which express the folate receptor at higher levels than IGROV-1 cells, and it was abolished if the cells were coincubated with excess folic acid to block folate receptor binding of ^{177}Lu-EC0800. Inhibition of cell viability through application of ^{177}Lu-EC0800 was enhanced if cells were coincubated with PMX (Fig. 1). Determination of the combination indices at different drug concentrations revealed that ^{177}Lu-EC0800 and PMX provided synergistic inhibitory effects on the viability of both tumor cell lines. It was observed that incubation of the cancer cells with PMX resulted in an accumulation of the cells in the G_1–S boundary or early S phase as previously reported (Supplementary Methods and Fig. S7; refs. 25 and 44). However, exposure of cells to ^{177}Lu-EC0800 showed a cell-cycle arrest in the G_2 –M phase, which is a common phenomenon in eukaryotic cells exposed to ionizing radiation (45). However, if the cancer cells were simultaneously exposed to ^{177}Lu-EC0800 and PMX the cell-cycle arrest in G_2–M phase was abrogated. Notably, the disruption of the radiation-induced G_2-checkpoint by chemotherapeutic agents (e.g., protein kinase inhibitors) was previously shown to sensitize cancer cells to radiation-induced apoptosis and cell death (46–48). This mechanism might also have been responsible for PMX-induced radiosensitization of KB and IGROV-1 cells. An increased apoptotic cell fraction was measured if the cells were treated with ^{177}Lu-EC0800 and PMX

Table 3. Results of the therapy studies with KB and IGROV-1 tumor-bearing mice using ^{177}Lu-EC0800 and/or PMX

Model I: KB tumor xenografts

Group	PMX (mg)	Radioactivity (MBq)	RTV day 17	TGI (%)	$TGDI_4$	Average survival time (%)
A	–	–	10.0 ± 2.7	–	1.0	–
B	$2 \times 0.8_{(ther)}$	–	9.8 ± 4.1	2.1	1.2	+22.5%
C	$1 \times 0.4_{(subther)}$	1 × 20	8.3 ± 3.5	16.9	1.4	+50.0%
D	$2 \times 0.8_{(ther)}$	1 × 20	5.0 ± 2.2	50.4	1.9	+75.0%

Model II: IGROV-1 tumor xenografts

Group	PMX (mg)	Radioactivity (MBq)	RTV day 17	TGI (%)	$TGDI_4$	Average survival time (%)
A	–	–	30.0 ± 14.9	0.0	1.0	–
B	$2 \times 0.8_{(ther)}$	–	27.9 ± 11.8	7.1	1.8	+0%
C	$1 \times 0.4_{(subther)}$	1 × 20	7.3 ± 3.9	75.8	2.6	+63.0%
D	$2 \times 0.8_{(ther)}$	1 × 20	2.0 ± 1.7	93.2	4.0	+100%

compared to the application of each of these therapeutics alone (Supplementary Methods and Fig. S8).

In vivo the preinjection of PMX improved the tissue distribution of ^{177}Lu-EC0800 dramatically by increasing the tumor-to-kidney ratio (Table 1). In an attempt to understand the underlying mechanism, the uptake of ^{3}H-PMX was determined in KB tumors and kidneys of mice. In the kidneys, we found a relatively high uptake 1 hour p.i. of ^{3}H-PMX, which was quickly cleared over time (Supplementary Fig. S5). These findings, together with the fact that PMX has a high affinity for the folate receptor (49), support our hypothesis of a competition among PMX and ^{177}Lu-EC0800 for folate receptor binding sites in the kidneys if PMX was injected about 1 hour before the radiofolate. In the tumor tissue, uptake of ^{3}H-PMX was low but retained over time. It has been reported previously that the tumor uptake of PMX is mediated primarily through carriers such as the reduced folate carrier and the proton-coupled folate transporter, whereas folate receptors play a minor role (50). This may explain the fact that PMX does not compete with the folate receptor–mediated accumulation of ^{177}Lu-EC0800 in tumor xenografts.

For the first time we were able to show in this study that PMX prevents damage to the kidneys by reducing renal accumulation of ^{177}Lu-EC0800. Analysis of plasma parameters and the results of SPECT studies using ^{99m}Tc-DMSA consistently confirmed normal kidney function in ^{177}Lu-EC0800-treated mice that had received a subtherapeutic amount of PMX. These findings unambiguously confirmed the beneficial role of PMX to prevent radionephropathy of radiofolate therapy.

Based on the *in vitro* results showing a synergistic effect of PMX and ^{177}Lu-EC0800 on the viability of tumor cells, it is likely that the anticancer effect of ^{177}Lu-EC0800 would be enhanced by coapplication of therapeutic amounts of PMX (2 × 0.8 mg, corresponding to 80% of the MTD; ref. 16). Therapy studies were conducted with KB (model I) and IGROV-1 tumor-bearing mice (model II) using ^{177}Lu-EC0800 combined with either subtherapeutic (0.4 mg/mouse) or therapeutic doses (e.g., 2 × 0.8 mg) of PMX. In both models, tumor growth delay was observed after application of ^{177}Lu-EC0800. Application of PMX_{ther} alone showed only minor inhibitory effects on growth of these tumor types. However, PMX_{ther} was able to enhance the anticancer effect of ^{177}Lu-EC0800 against both KB and IGROV-1 tumor xenografts. Also, an increased survival time was achieved if ^{177}Lu-EC0800 and PMX were combined compared to the result obtained with each of these agents applied as monotherapy.

With this study we were able to show the proposed dual effect of PMX in combination with folate receptor targeted radionuclide therapy using ^{177}Lu-EC0800. On one hand, PMX at subtherapeutic and therapeutic amounts effectively reduced renal uptake of ^{177}Lu-EC0800 and therewith prevented long-term radionephropathy (Table 1, Fig. 2). On the other hand, the application of PMX_{ther} enhanced the tumor growth delay induced by ^{177}Lu-EC0800. The interplay of the proposed drug combination is absolutely unique. Therefore, we believe that combining PMX with ^{177}Lu-folate therapy warrants further preclinical investigations. Assuming the kidney-reducing effect of PMX could be confirmed also in man, the combined application of therapeutic radiofolates and PMX has a potential translational impact. Such a therapy protocol would be particularly interesting for the treatment of non–small cell lung cancer, which frequently shows folate receptor overexpression and for which PMX is a Food and Drug Administration-approved indication.

Disclosure of Potential Conflicts of Interest

No potential conflicts of interest were disclosed.

Authors' Contributions

Conception and design: J. Reber, C. Müller
Development of methodology: J. Reber, C. Müller
Acquisition of data (provided animals, acquired and managed patients, provided facilities, etc.): J. Reber, S. Haller, C. Müller
Analysis and interpretation of data (e.g., statistical analysis, biostatistics, computational analysis): J. Reber, C.P. Leamon, C. Müller
Writing, review, and/or revision of the manuscript: J. Reber, S. Haller, C.P. Leamon, C. Müller
Administrative, technical, or material support (i.e., reporting or organizing data, constructing databases): J. Reber, S. Haller
Study supervision: C. Müller

Acknowledgments

The authors thank Prof. R. Schibli for helpful advice with regard to the design of this study and for reviewing the manuscript. The authors are grateful for technical assistance of the experiments by N. Romano.

Grant Support

C. Müller was financially supported by the Swiss National Science Foundation (Ambizione, Grants PZ00P3_121772 and PZ00P3_138834), S. Haller was supported by the Swiss Cancer League (KLS-02762-02-2011), and J. Reber was supported by COST-BM0607 (C08.0026).

The costs of publication of this article were defrayed in part by the payment of page charges. This article must therefore be hereby marked *advertisement* in accordance with 18 U.S.C. Section 1734 solely to indicate this fact.

Received May 30, 2013; revised August 29, 2013; accepted September 8, 2013; published OnlineFirst September 12, 2013.

References

1. Zoller F, Eisenhut M, Haberkorn U, Mier W. Endoradiotherapy in cancer treatment—basic concepts and future trends. Eur J Pharmacol 2009;625:55–62.
2. Kam BL, Teunissen JJ, Krenning EP, de Herder WW, Khan S, van Vliet EI, et al. Lutetium-labelled peptides for therapy of neuroendocrine tumours. Eur J Nucl Med Mol Imaging 2012;39 Suppl 1:S103–12.
3. Tomblyn M. Radioimmunotherapy for B-cell non-Hodgkin lymphomas. Cancer Contr 2012;19:196–203.
4. Parker N, Turk MJ, Westrick E, Lewis JD, Low PS, Leamon CP. Folate receptor expression in carcinomas and normal tissues determined by a quantitative radioligand binding assay. Anal Biochem 2005;338:284–93.
5. Low PS, Kularatne SA. Folate-targeted therapeutic and imaging agents for cancer. Curr Opin Chem Biol 2009;13:256–62.
6. Salazar MD, Ratnam M. The folate receptor: what does it promise in tissue-targeted therapeutics? Cancer Metastasis Rev 2007;26:141–52.
7. Dosio F, Milla P, Cattel L. EC-145, a folate-targeted Vinca alkaloid conjugate for the potential treatment of folate receptor-expressing cancers. Curr Opin Investig Drugs 2010;11:1424–33.
8. Pribble P, Edelman MJ. EC145: a novel targeted agent for adenocarcinoma of the lung. Expert Opin Investig Drugs 2012;21:755–61.
9. Holm J, Hansen SI, Hoiermadsen M, Bostad L. A high-affinity folate binding-protein in proximal tubule cells of human kidney. Kidney Int 1992;41:50–5.
10. Sandoval RM, Kennedy MD, Low PS, Molitoris BA. Uptake and trafficking of fluorescent conjugates of folic acid in intact kidney determined using intravital two-photon microscopy. Am J Physiol Cell Physiol 2004;287:C517–26.
11. Müller C, Reddy JA, Leamon CP, Schibli R. Effects of the antifolates pemetrexed and CB3717 on the tissue distribution of ^{99m}Tc-EC20 in xenografted and syngeneic tumor-bearing mice. Mol Pharm 2010;7:597–604.
12. Müller C, Schibli R, Krenning EP, de Jong M. Pemetrexed improves tumor selectivity of ^{111}In-DTPA-folate in mice with folate receptor-positive ovarian cancer. J Nucl Med 2008;49:623–9.
13. Müller C, Mindt TL, de Jong M, Schibli R. Evaluation of a novel radiofolate in tumour-bearing mice: promising prospects for folate-based radionuclide therapy. Eur J Nucl Med Mol Imaging 2009;36:938–46.
14. Müller C, Brühlmeier M, Schubiger AP, Schibli R. Effects of antifolate drugs on the cellular uptake of radiofolates *in vitro* and *in vivo*. J Nucl Med 2006;47:2057–64.
15. Müller C, Schibli R, Forrer F, Krenning EP, de Jong M. Dose-dependent effects of (anti)folate preinjection on ^{99m}Tc-radiofolate uptake in tumors and kidneys. Nucl Med Biol 2007;34:603–8.
16. Müller C, Reber J, Schlup C, Leamon CP, Schibli R. *In vitro* and *in vivo* evaluation of an innocuous drug cocktail to improve the quality of folic acid targeted nuclear imaging in preclinical research. Mol Pharm 2013;10:967–74.
17. Vogelzang NJ, Rusthoven JJ, Symanowski J, Denham C, Kaukel E, Ruffie P, et al. Phase III study of pemetrexed in combination with cisplatin versus cisplatin alone in patients with malignant pleural mesothelioma. J Clin Oncol 2003;21:2636–44.
18. Hazarika M, White RM, Johnson JR, Pazdur R. FDA drug approval summaries: pemetrexed (Alimta). Oncologist 2004;9:482–8.
19. Rollins KD, Lindley C. Pemetrexed: a multitargeted antifolate. Clin Ther 2005;27:1343–82.
20. Hanauske AR, Chen V, Paoletti P, Niyikiza C. Pemetrexed disodium: a novel antifolate clinically active against multiple solid tumors. Oncologist 2001;6:363–73.
21. Morotti M, Valenzano Menada M, Venturini PL, Mammoliti S, Ferrero S. Pemetrexed disodium in ovarian cancer treatment. Expert Opin Investig Drugs 2012;21:437–49.
22. Monnerat C, Le Chevalier T. Review of the pemetrexed and gemcitabine combination in patients with advanced-stage non-small cell lung cancer. Ann Oncol 2006;17 Suppl 5:v86–90.
23. Govindan R, Bogart J, Stinchcombe T, Wang X, Hodgson L, Kratzke R, et al. Randomized phase II study of pemetrexed, carboplatin, and thoracic radiation with or without cetuximab in patients with locally advanced unresectable non-small-cell lung cancer: cancer and Leukemia Group B trial 30407. J Clin Oncol 2011;29:3120–5.
24. Seiwert TY, Connell PP, Mauer AM, Hoffman PC, George CM, Szeto L, et al. A phase I study of pemetrexed, carboplatin, and concurrent radiotherapy in patients with locally advanced or metastatic non-small cell lung or esophageal cancer. Clin Cancer Res 2007;13:515–22.
25. Bischof M, Weber KJ, Blatter J, Wannenmacher M, Latz D. Interaction of pemetrexed disodium (ALIMTA, multitargeted antifolate) and irradiation *in vitro*. Int J Radiat Oncol Biol Phys 2002;52:1381–8.
26. Huber PE, Bischof M, Jenne J, Heiland S, Peschke P, Saffrich R, et al. Trimodal cancer treatment: beneficial effects of combined antiangiogenesis, radiation, and chemotherapy. Cancer Res 2005;65:3643–55.
27. Yoshida D, Ebara T, Sato Y, Kaminuma T, Takahashi T, Asao T, et al. Interaction of radiation and pemetrexed on a human malignant mesothelioma cell line *in vitro*. Anticancer Res 2011;31:2847–51.
28. Shewach DS, Lawrence TS. Antimetabolite radiosensitizers. J Clin Oncol 2007;25:4043–50.
29. Müller C, Vlahov IR, Santhapuram HK, Leamon CP, Schibli R. Tumor targeting using ^{67}Ga-DOTA-Bz-folate—investigations of methods to improve the tissue distribution of radiofolates. Nucl Med Biol 2011;38:715–23.
30. Müller C, Struthers H, Winiger C, Zhernosekov K, Schibli R. DOTA conjugate with an albumin-binding entity enables the first folic acid-targeted ^{177}Lu-radionuclide tumor therapy in mice. J Nucl Med 2013;54:124–31.
31. Weitman SD, Lark RH, Coney LR, Fort DW, Frasca V, Zurawski VR, et al. Distribution of the folate receptor GP38 in normal and malignant cell lines and tissues. Cancer Res 1992;52:3396–401.

32. Müller C, Schubiger PA, Schibli R. *In vitro* and *in vivo* targeting of different folate receptor-positive cancer cell lines with a novel ^{99m}Tc-radiofolate tracer. Eur J Nucl Med Mol Imaging 2006;33:1162–70.
33. Hattori Y, Maitani Y. Folate-linked nanoparticle-mediated suicide gene therapy in human prostate cancer and nasopharyngeal cancer with herpes simplex virus thymidine kinase. Cancer Gene Ther 2005;12:796–809.
34. Franken NA, Rodermond HM, Stap J, Haveman J, van Bree C. Clonogenic assay of cells *in vitro*. Nat Protoc 2006;1:2315–9.
35. Mosmann T. Rapid colorimetric assay for cellular growth and survival: application to proliferation and cytotoxicity assays. J Immunol Methods 1983;65:55–63.
36. Reber J, Struthers H, Betzel T, Hohn A, Schibli R, Müller C. Radioiodinated folic acid conjugates: evaluation of a valuable concept to improve tumor-to-background contrast. Mol Pharm 2012;9:1213–21.
37. Chou TC. Theoretical basis, experimental design, and computerized simulation of synergism and antagonism in drug combination studies. Pharmacol Rev 2006;58:621–81.
38. Mathias CJ, Wang S, Lee RJ, Waters DJ, Low PS, Green MA. Tumor-selective radiopharmaceutical targeting via receptor-mediated endocytosis of gallium-67-deferoxamine-folate. J Nucl Med 1996;37:1003–8.
39. Forrer F, Valkema R, Bernard B, Schramm NU, Hoppin JW, Rolleman E, et al. *In vivo* radionuclide uptake quantification using a multi-pinhole SPECT system to predict renal function in small animals. Eur J Nucl Med Mol Imaging 2006;33:1214–7.
40. Leamon CP, Reddy JA, Vlahov IR, Westrick E, Parker N, Nicoson JS, et al. Comparative preclinical activity of the folate-targeted Vinca alkaloid conjugates EC140 and EC145. Int J Cancer 2007;121:1585–92.
41. Sanceau J, Poupon MF, Delattre O, Sastre-Garau X, Wietzerbin J. Strong inhibition of Ewing tumor xenograft growth by combination of human interferon-α or interferon-β with ifosfamide. Oncogene 2002;21:7700–9.
42. Jiang L, Zeng X, Wang Z, Chen Q. Cell line cross-contamination: KB is not an oral squamous cell carcinoma cell line. Eur J Oral Sci 2009;117:90–1.
43. Weyer K, Nielsen R, Petersen SV, Christensen EI, Rehling M, Birn H. Renal uptake of ^{99m}Tc-dimercaptosuccinic acid is dependent on normal proximal tubule receptor-mediated endocytosis. J Nucl Med 2013;54:159–65.
44. Tonkinson JL, Worzalla JF, Teng CH, Mendelsohn LG. Cell cycle modulation by a multitargeted antifolate, LY231514, increases the cytotoxicity and antitumor activity of gemcitabine in HT29 colon carcinoma. Cancer Res 1999;59:3671–6.
45. Maity A, McKenna WG, Muschel RJ. The molecular basis for cell cycle delays following ionizing radiation: a review. Radiother Oncol 1994;31:1–13.
46. Yao SL, Akhtar AJ, McKenna KA, Bedi GC, Sidransky D, Mabry M, et al. Selective radiosensitization of p53-deficient cells by caffeine-mediated activation of p34cdc2 kinase. Nat Med 1996;2:1140–3.
47. Busby EC, Leistritz DF, Abraham RT, Karnitz LM, Sarkaria JN. The radiosensitizing agent 7-hydroxystaurosporine (UCN-01) inhibits the DNA damage checkpoint kinase hChk1. Cancer Res 2000;60:2108–12.
48. Wang Y, Li J, Booher RN, Kraker A, Lawrence T, Leopold WR, et al. Radiosensitization of p53 mutant cells by PD0166285, a novel G_2 checkpoint abrogator. Cancer Res 2001;61:8211–7.
49. Westerhof GR, Schornagel JH, Kathmann I, Jackman AL, Rosowsky A, Forsch RA, et al. Carrier- and receptor-mediated transport of folate antagonists targeting folate-dependent enzymes: correlates of molecular-structure and biological activity. Mol Pharmacol 1995;48:459–71.
50. Zhao R, Qiu A, Tsai E, Jansen M, Akabas MH, Goldman ID. The proton-coupled folate transporter: impact on pemetrexed transport and on antifolates activities compared with the reduced folate carrier. Mol Pharmacol 2008;74:854–62.